Theoretical realization and application of parity-time-symmetric oscillators in a quantum regime

Wenlin Li, Chong Li, and Heshan Song*

School of Physics and Optoelectronic Engineering, Dalian University of Technology, Dalian 116024, China

(Received 17 August 2016; published 14 February 2017)

In the existing parity-time ($\mathcal{PT}$) symmetry with the balanced gain and loss, the gain is derived from semiclassical but not full quantum theories, which significantly restricts the applications of $\mathcal{PT}$ symmetry in quantum fields. In this work, we propose and analyze a theoretical scheme to realize full quantum oscillator $\mathcal{PT}$ symmetry. The quantum gain is provided by a dissipation optical cavity with a blue-detuned laser field. After adiabatically eliminating the cavity modes, we give an effective master equation, which is a complete quantum description compared with the non-Hermitian Hamiltonian, to reveal the quantum behaviors of such a gain oscillator. This kind of $\mathcal{PT}$ symmetry can eliminate the dissipation effect in the quantum regime. As an example, we apply $\mathcal{PT}$-symmetric oscillators to enhance optomechanically induced transparency.

DOI: 10.1103/PhysRevA.95.023827

I. INTRODUCTION

In recent years, the notion of parity-time ($\mathcal{PT}$) symmetry has attracted considerable interest due to its potential applications in the fields of quantum optics and quantum information processing (QIP) [1–4]. Since Bender and Boettcher proved that a $\mathcal{PT}$-symmetric non-Hermitian Hamiltonian ($\hat{H}^\dagger \neq \hat{H}, [\hat{H}, PT] = 0$) can also have a real eigenvalue spectrum [5,6], realizing $\mathcal{PT}$-symmetric complex quantum systems has become a rapidly developing issue in both theoretical and experimental studies [7–13]. Currently, non-Hermitian-based complex quantum mechanics is still debated [14]; however, it is significant to test the $\mathcal{PT}$ symmetry in open quantum systems or optical systems. Recent experiments have already demonstrated $\mathcal{PT}$-symmetry behaviors in a variety of physical systems [15–19]. Among them, a simple and intuitive scheme is to link two quantum open systems with gain and loss [2,10,16,17,20]. As reported in Refs. [2,10], experimentalists observed that a mode splitting between two supermodes will occur with degenerate effective dissipations once the coupling intensity passes through the exceptional point (EP). Ideally, the balanced gain and loss make the eigenvalues appear on the real axis. The system supermodes perform similar to a closed quantum system in this case, and some environmental damage effects can be suppressed by quantum gain. So far, a similar mechanism has already been applied in several quantum investigations, including enhancing optics nonlinearity [15,21], intensifying photon blockade [16], and realizing quantum chaos [17] by using an extra optical gain.

Although $\mathcal{PT}$ symmetry has made progress in optimizing the QIP scheme, it is regrettable that the common non-Hermitian Hamiltonian is not a complete quantum description for open gain or loss quantum systems [14]. In previous works, the gains were generally introduced by classical amplification effects (e.g., parameter amplifier or erbium-doped waveguide or microcavity amplifiers) [2,10,16,17,20–22]. Correspondingly, a dissipation non-Hermitian Hamiltonian can be deduced by adopting a Markovian quantum master equation after neglecting its jump term or by utilizing quantum Langevin equations without input operators. However, it still remains difficult to discuss the quantum effect of such a $\mathcal{PT}$-symmetric system when our focus is not restricted to the semiclassical level [16,17,20–22]. Realizing a gain and then realizing a $\mathcal{PT}$-symmetric system in the quantum regime become natural desires in the research field of $\mathcal{PT}$ symmetry.

In the past decade, quantized mechanical oscillators have already provided critical resources for studying basic quantum theory and QIP [23–27]. It is well known that oscillators can constitute so-called optomechanical systems via the radiation pressure interaction between electromagnetic and mechanical systems [28]. Because of this radiation pressure, cavity optomechanics plays an indispensable role in the QIP scheme, and an instructive discovery is that the oscillators can be enhanced and heated (suppressed and cooled) under the blue (red) sideband by tuning the detuning of the driving fields [29–31]. This implies that the oscillator will function to obtain an effective gain in this case [32], and more importantly, a quantum description for this gain can be found after eliminating the cavity field.

In this study, we adopt the above idea to realize $\mathcal{PT}$-symmetric oscillators in the quantum regime. After adiabatically eliminating the cavity modes, we give an effective master equation to describe the effective gain of the oscillator. For some particular quantum states (e.g., Gaussian state), this master equation is strict, which indicates that some quantum effects that cannot be calculated accurately by the non-Hermitian Hamiltonian can be discussed perfectly in this $\mathcal{PT}$-symmetry system. In contrast to Ref. [32], here, the quantum properties can be considered without reconsidering the eliminated system. Therefore, our $\mathcal{PT}$-symmetric oscillators can be applied in existing QIP schemes more simply and intuitively. As an example, we apply $\mathcal{PT}$-symmetric oscillators to enhance optomechanically induced transparency (OMIT). We believe this system can provide a promising platform for QIP.

II. REALIZATION OF OSCILLATOR GAIN IN THE QUANTUM REGIME

Let us start by focusing on the realization of oscillator gain in the quantum regime. As shown in Fig. 1(a), we consider a typical optomechanical system consisting of a mechanical

*hssong@dlut.edu.cn

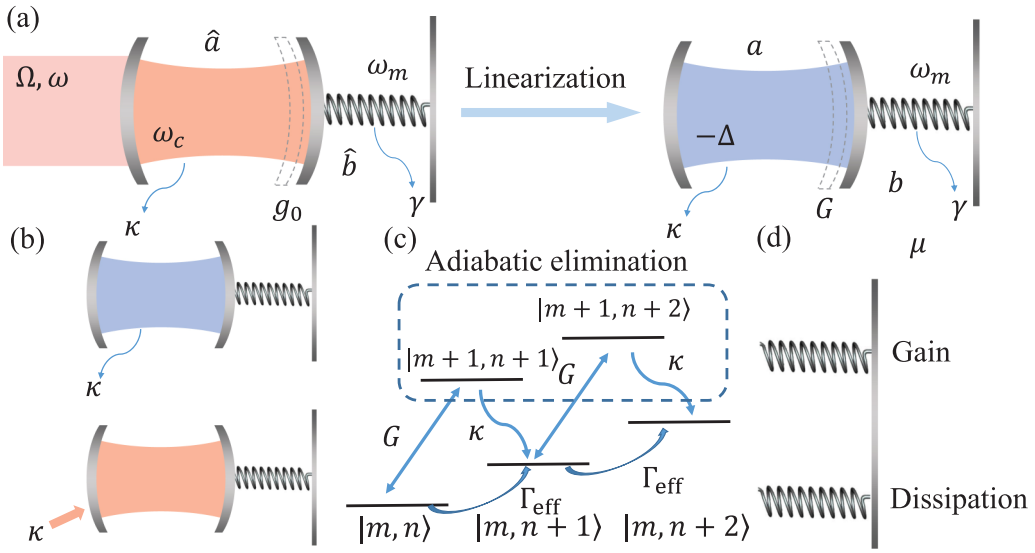

FIG. 1. (a) A typical dissipative optomechanical system and its corresponding model after linearization. This type of system can also be considered a hybrid system consisting of a transmission line resonator and a superconducting qubit. (b) Two schemes for realizing oscillator gain, corresponding to a dissipative cavity optomechanical system under the blue sideband and a gain cavity optomechanical system under the red sideband, respectively. (c) Level diagram of the blue sideband. Here, $|n,m\rangle$ denotes the state of n photons and m phonons in the displaced frame. (d) A gain and a dissipation mutually interacting through a phonon tunneling term of intensity μ.

oscillator and a Fabry-Pérot resonator. For the convenience of studying the effects in the gain process, we transform the Hamiltonian into a displaced oscillator representation in the strong driving condition, which, along with the corresponding energy-level structure, is shown in Fig. 1(c). We note that there is a quantum backaction heating process under the blue-resolved sideband ($\Delta = \omega_m$): the heat-exchange process transits the oscillator from state $|m,n\rangle$ to $|m+1,n+1\rangle$, and a strong optical dissipation causes the oscillator to transit irreversibly from state $|m+1,n+1\rangle$ to $|m,n+1\rangle$. After eliminating the cavity modes, this process is equivalent to gaining the oscillator from $|n\rangle$ to $|n+1\rangle$ with a gain rate $|\Gamma_{\text{eff}}|$ [see Fig. 1(b)]. Because the gain comes from the eliminated cavity mode whose quantum properties can be completely described by a certain Hamiltonian, it can be regarded as a full quantum but not a semiclassical theory similar to previous works.

In a general dissipative system, the low-temperature bath makes the oscillator decay from $|n\rangle$ to $|n-1\rangle$; that is, it is an inverse process compared with the effective gain. Therefore, under appropriate parameters, the gain can be well balanced with dissipation and can provide the potential to achieve $\mathcal{PT}$ symmetry. For example, if we consider two identical oscillators that correspond to gain and dissipation and interact mutually through phonon tunneling, then the Hamiltonians can exhibit a real eigenvalue spectrum, and the oscillators are transited into the $\mathcal{PT}$-symmetric phase.

Now we analyze the above discussion quantitatively; the total Hamiltonian corresponding to the optomechanical system in Fig. 1(a) is ($\hbar = 1$) [28,29]

$$H = -\Delta\hat{a}^\dagger\hat{a} + \omega\hat{b}^\dagger\hat{b} + g\hat{a}^\dagger\hat{a}(\hat{b} + \hat{b}^\dagger) + (\Omega\hat{a}^\dagger + \Omega^*\hat{a}^\dagger) \quad (1)$$

after a frame rotation. Here, $\Delta = \omega - \omega_c$ is the input cavity detuning; $\hat{a}$ ($\hat{b}$) is the annihilation operator of the optical (mechanical) mode with the corresponding angular resonance frequency ω_c (ω_m). g is the single-photon optomechanical coupling rate, and $\Omega = \sqrt{\kappa_{\text{ex}}P/(\hbar\omega)}e^{i\phi}$ is the driving intensity, with the input laser power P and the initial input laser phase (cavity coupling) ϕ (κ_{ex}). Based on Eq. (1), the quantum Langevin equations can be expressed as

$$\begin{aligned}\dot{\hat{a}} &= \left(i\Delta - \frac{\kappa}{2}\right)\hat{a} - ig\hat{a}(\hat{b} + \hat{b}^\dagger) - i\Omega - \hat{\xi},\\ \dot{\hat{b}} &= \left(-i\omega_m - \frac{\gamma}{2}\right)\hat{b} - ig\hat{a}^\dagger\hat{a} - \sqrt{\gamma}b_{\text{in}},\end{aligned} \quad (2)$$

where γ denotes the intrinsic oscillator dissipation. $\kappa = \kappa_{\text{ex}} + \kappa_0$ is the total cavity dissipation rate, where κ_0 is the intrinsic cavity dissipation; $\hat{\xi} = \sqrt{\kappa_{\text{ex}}}a_{\text{in,ex}} + \sqrt{\kappa_0}a_{\text{in},0}$ and b_{in} are the input noise operators describing the dissipative effects, including intrinsic cavity dissipation, external cavity dissipation, and mechanical dissipation [29]. If the optomechanical coupling is quite weak in the quantum regime, the motion of the oscillator and optical field can be regarded as perturbations on their respective steady states, implying that each operator in Eq. (2) can be rewritten as a sum of a c-number steady-state value and a perturbation operator, i.e., $\hat{a} = \alpha + a$ and $\hat{b} = \beta + b$. Substituting these relations into Langevin equations and neglecting the high-order perturbation terms, the system can be linearized by separating the steady states and perturbation components, and then the dynamics of the perturbation operator will satisfy a linear Hamiltonian (see Appendix A for details),

$$H = -\Delta' a^\dagger a + \omega b^\dagger b + Ga^\dagger b^\dagger + G^* ab, \quad (3)$$

under the blue-sideband condition $\Delta' > 0$ [29] [system at the top of Fig. 1(b)]. Here, we assume $\Delta' = \Delta - 2g\text{Re}(\beta) \simeq \Delta$. Unlike the common linearization process, in which c numbers are set as the operator expectation values, here, $\langle a\rangle = 0$ and $\langle b\rangle = 0$ are not always tenable in this case. According to

Eq. (3), the master equation reads

$$\dot{\rho} = -i[H,\rho] + \frac{\kappa}{2}\mathcal{L}[a]\rho + \frac{\gamma}{2}(n_{\rm th}+1)\mathcal{L}[b]\rho + \frac{\gamma}{2}n_{\rm th}\mathcal{L}[b^\dagger]\rho, \tag{4}$$

where $\mathcal{L}[o]\rho = (2o\rho o^\dagger - o^\dagger o\rho - \rho o^\dagger o)$ is the standard form of the Lindblad superoperator. By making premultiplications with mechanical quantity operators on both sides of Eq. (4), evolutions of the system dynamics can be described by a set of partial differential equations instead of solving all elements of the density matrix ρ. Here, we consider only the first- and second-order mechanical quantities for convenience, and the linear Hamiltonian ensures dynamic equations are closed in each order. Using the master equation, we can get the following differential equations of first-order mechanical quantities by performing premultiplication with each observable operator:

$$\frac{d}{dt}\langle a\rangle = \left(i\Delta - \frac{\kappa}{2}\right)\langle a\rangle - iG\langle b\rangle^*,$$
$$\frac{d}{dt}\langle b\rangle = \left(-i\omega_m - \frac{\gamma}{2}\right)\langle b\rangle - iG\langle a\rangle^*. \tag{5}$$

Correspondingly, the second-order mechanical quantities are described by

$$\frac{d}{dt}\langle a^\dagger a\rangle = -\kappa\langle a^\dagger a\rangle - i[G\langle ab\rangle^* - G^*\langle ab\rangle],$$
$$\frac{d}{dt}\langle b^\dagger b\rangle = -\gamma\langle b^\dagger b\rangle + \gamma n_{\rm th} - i[G\langle ab\rangle^* - G^*\langle ab\rangle],$$
$$\frac{d}{dt}\langle ab\rangle = \left[i(\Delta-\omega_m) - \frac{\kappa+\gamma}{2}\right]\langle ab\rangle - iG[\langle a^\dagger a\rangle + \langle b^\dagger b\rangle + 1]. \tag{6}$$

Here, $\langle\cdots\rangle$ implies taking the expectation value with respect to the density matrix of the quantum system. Note that, in the above calculations, a cutoff of the density matrix is not necessary and the solutions are exact. Here, for convenience in following discussion, we define a constant factor

$$\eta = \frac{4|G|^2}{4(\Delta-\omega_m)^2+\kappa^2} \tag{7}$$

to describe the optomechanical-induced modifications of the oscillator dynamics. After an iteration, the evolution equations of the first- and second-order mechanical quantities can be simplified, respectively, as

$$\frac{d}{dt}\langle b\rangle = \left(-i\omega_{\rm eff} - \frac{\Gamma_{\rm eff}}{2}\right)\langle b\rangle \tag{8}$$

and

$$\frac{d}{dt}\langle b^\dagger b\rangle = -\Gamma_{\rm eff}\langle b^\dagger b\rangle + \gamma n_{\rm th} + \eta\kappa \tag{9}$$

by adiabatically eliminating the optical-field freedom. The coefficients of $\langle b\rangle$ and $\langle b^\dagger b\rangle$ on the right-hand sides of Eqs. (8) and (9) correspond to the contributions of the non-Hermitian Hamiltonian

$$H_{\rm eff} = \left(\omega_{\rm eff} - i\frac{\Gamma_{\rm eff}}{2}\right)b^\dagger b, \tag{10}$$

with an effective frequency $\omega_{\rm eff} = \omega_m + \eta(\Delta-\omega_m)$ and an effective dissipation $\Gamma_{\rm eff} = \gamma - \eta\kappa$. Moreover, the last two terms in Eq. (9) are modified noise terms caused by jump operators in the master equation. Therefore, the mechanical oscillator can finally be described by the following master equation:

$$\dot{\rho} = -i[\omega_{\rm eff}b^\dagger b,\rho] + \frac{\Gamma_{\rm eff}}{2}(n'_{\rm th}+1)\mathcal{L}[b]\rho + \frac{\Gamma_{\rm eff}}{2}n'_{\rm th}\mathcal{L}[b^\dagger]\rho, \tag{11}$$

where the modified thermal phonon number is

$$n'_{\rm th} = \frac{\gamma n_{\rm th} + \eta\kappa}{\Gamma_{\rm eff}} \tag{12}$$

and the modified initial conditions of the oscillator

$$\langle b\rangle'_{t_0} \simeq \sqrt{\langle b^\dagger b\rangle'_{t_0}},$$
$$\langle b^\dagger b\rangle'_{t_0} = (1+2\eta)\langle b^\dagger b\rangle_{t_0} + \eta\langle a^\dagger a\rangle_{t_0} - \frac{2\eta(\Delta-\omega_m)}{G^*}\langle ab\rangle_{t_0} \tag{13}$$

describe an optomechanical-induced energy translation.

We emphasize here that the only approximation used in the above deduction is the elimination of the optical field. Therefore, unlike the non-Hermitian Hamiltonian, Eq. (11) contains all properties of the second-order expectation values of the oscillators ($\langle b^\dagger b\rangle$, $\langle bb\rangle$, and $\langle b^\dagger b^\dagger\rangle$), which indicate that some quantum properties, e.g., quantum fluctuation, can also be discussed by using Eq. (11). Because we iterate only the first- and second-order expectation value equations, Eq. (11) is still incomplete if it is used to solve density-matrix or high-order expectation values (e.g., $\langle b^\dagger bb\rangle$). If $\Delta \gg \omega_m$, the constant factor can be approximated as $\eta = 4|G|^2/(4\Delta^2+\kappa^2)$, which is the same conclusion as that of treating the auxiliary mode as a steady state [33]. However, linearization approximation will limit the conditions occurring for such kinds of parameters in the optomechanical system.

We note that the effective dissipation is reduced by the factor $\eta\kappa = 4|G^2|\kappa/[4(\Delta-\omega_m)^2+\kappa^2]$ due to the heating process. If the linearized optomechanical coupling strength satisfies $|G^2| > \gamma[4(\Delta-\omega_m)^2+\kappa^2]/\kappa$, $\Gamma_{\rm eff}$ will no longer be a positive but a negative dissipation. The non-Hermitian Hamiltonian now describes a gain effect, and the mechanical oscillations display antidamping.

In Fig. 2, we show the effective dissipation rates of the system under different parameters after adiabatic elimination. One can observe directly that the effective dissipation can take on a negative value, which corresponds to a gain effect. Under certain parameters, it can be found from Fig. 2(a) that $\Gamma_{\rm eff}/\gamma = -1$ and the quantum dissipation is completely balanced by such a gain. To demonstrate the accuracy of the approximation, we plot Figs. 2(b) and 2(c) to compare, respectively, the evolutions of the first- and second-order mechanical quantities in the approximate system and original system; it is known that two mechanical quantities gradually exhibit remarkably consistent evolutions. For a Gaussian state, both the first- and second-order mechanical quantities are accurately described, meaning that it is a complete quantum description. In Fig. 2(d), we plot the Gaussian fidelity [34,35]

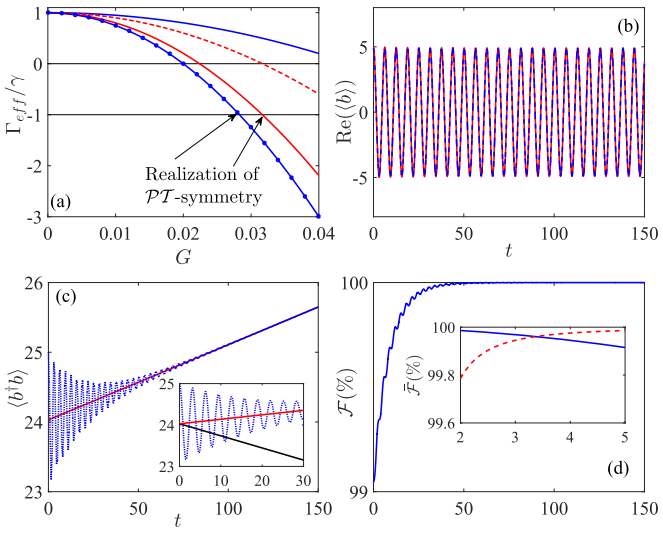

FIG. 2. (a) Changes in the effective dissipation coefficient with varied linear coupling coefficient G. Comparisons of evolutions corresponding to (b) the first-order and (c) second-order mechanical quantities. Here, the blue dotted lines denote mechanical quantities of the original system, and red solid lines denote the approximate system after adiabatic elimination. The black line in the inset is the evolution without bath correction. (d) The fidelity between the oscillator states corresponds to the original and approximate systems. The inset in (d) shows the time-averaged fidelities with varied coupling coefficient G (blue solid line) and the detuning Δ (red dotted line). Here, the horizontal axis is $100G$ (Δ) for the blue (red) line. In this simulation, we set $\omega_m = 1$ as the unit; the other dimensionless parameters are $\kappa = 0.1$, $n_b = 1000$. In (a), we set $\Delta = 2$ (3) for the red lines (blue lines) and $\gamma = 5\times10^{-5}$ (10^{-4}, 10^{-5}) for the solid line (dashed line, line with circles). In (b), (c), and (d), we set $\gamma = 10^{-5}$, $G = 0.04$ and $\Delta = 3$. The blue line in the inset in (d) corresponds to $\Delta = 3$, and the red line is under $G = 0.04$.

to illustrate that this description is complete and quantum due to $\mathcal{F} \to 100\%$, which indicates that it does not need to reconsider the eliminated system to obtain the system's quantum properties, like in Ref. [32], and that the physical processes in our picture are more intuitive.

Let us reexamine the effective bath phonon number in Eq. (12). A negative dissipation rate will change the heat-flow direction between the system and the bath, and a modified bath phonon number can also change the polarity of the phonon-number difference. Such double corrections ensure the correct direction of the heat flow. In the inset of Fig. 2(c), we show the system evolution corresponding to an incorrect heat-flow direction without correcting the bath phonon number. It shows that the system that should be heated is cooled, which implies that effective dissipation alone is not enough for the quantum description of the $\mathcal{PT}$-symmetric system.

III. $\mathcal{PT}$-SYMMETRIC OSCILLATOR WITH EFFECTIVE GAIN

Up to now, we have discussed a technique that can realize oscillator gain, and it is potentially useful in a wide range of phononic engineering systems, e.g., producing coherent phonon lasing. Instead of this, here, we study its impact on a $\mathcal{PT}$-symmetric oscillator. Generally, a $\mathcal{PT}$-symmetric system can be achieved by connecting a passive system and a positive system [see Fig. 1(d)] with a linear phonon coupling. The non-Hermitian Hamiltonian corresponding to such a system can be expressed as

$$H = \left(\omega - i\frac{\gamma}{2}\right)b_1^\dagger b_1 + \left(\omega + i\frac{\gamma'}{2}\right)b_2^\dagger b_2 + \mu(b_1^\dagger b_2 + \text{H.c.}), \tag{14}$$

where γ is an ordinary oscillator dissipation and $\gamma' = -\Gamma_{\text{eff}}$ denotes the quantum gain of the oscillator. Based on Eq. (14), the corresponding eigenvalues can be calculated as

$$\lambda_\pm = \omega - \frac{i(\gamma - \gamma')}{4} \pm \sqrt{\mu^2 - \left(\frac{\gamma + \gamma'}{4}\right)^2}, \tag{15}$$

and their real and imaginary parts correspond to effective frequency and dissipation, respectively. Equation (15) reflects that the system will be divided into two dynamic phases by $\mu = (\gamma + \gamma')/4$. When $\mu < (\gamma + \gamma')/4$, the third term in Eq. (15) will be a pure imaginary number, which leads to two different dissipation coefficients. Conversely, $\mu > (\gamma + \gamma')/4$ makes the system have a degenerated effective dissipation rate $(\gamma - \gamma')/2$ with resolved normal-mode splitting. In particular, $\lambda_\pm$ can both be real numbers under the condition $\gamma = \gamma'$, and the non-Hermitian Hamiltonian in this case is $\mathcal{PT}$ symmetric.

Physically, once the coupling intensity μ is weak enough to support energy transfer from the active oscillator to the passive oscillator, the field localization will induce the dynamical accumulation of the acoustical energy in the passive oscillator. This accumulated energy will not be able to balance dissipation effectively, which causes the whole system to lose its $\mathcal{PT}$ symmetry and come into the $\mathcal{PT}$-symmetry-breaking phase. With the gradually enhanced μ, the stronger phonon-tunneling effects will replace the localization gain (decay) effects in each oscillator. The oscillator dynamics at this time show more collective behavior as supermodes; simultaneously, the system enters into the $\mathcal{PT}$-symmetry phase because the gain and dissipation of each supermode are balanced. Therefore, $\mu = (\gamma + \gamma')/4$ is exactly the exceptional point transforming from the $\mathcal{PT}$-symmetric phase ($\mathcal{PT}$SP) to the $\mathcal{PT}$-symmetry-breaking phase ($\mathcal{PT}$BP).

In Figs. 3(a) and 3(b), we plot $\lambda_\pm$ as a function of μ to show the mode splitting and degenerate dissipation in the $\mathcal{PT}$SP regime more intuitively. Figure 3 also illustrates that the bifurcations of real and imaginary parts of the eigenvalues are still similar to the $\mathcal{PT}$SP and $\mathcal{PT}$BP for the unbalanced case, in which the loss and gain parameters γ and γ' are unequal. This case should be regarded as a physically realistic scenario, while $\gamma = \gamma'$ is an idealization; that is, a closed $\mathcal{PT}$-symmetric system is placed in a hot bath with an effective dissipation rate $(\gamma - \gamma')/2$ [36,37]. In Figs. 3(c) and 3(d), we plot the dynamic behaviors of the two oscillators to investigate the transitions of $\mathcal{PT}$SP and $\mathcal{PT}$BP. When $\mu = \gamma + \gamma'$, the two oscillators are in the $\mathcal{PT}$SP regime, shown in Fig. 3(c), and an obvious energy exchange process occurs; that is, the amplitude of each oscillator is intensified and weakened alternately. Two amplitudes have identical boundaries (roughly $[-4,4]$), and the evolution of each oscillator is stable within its own boundary. This indicates that the energy gain and dissipation

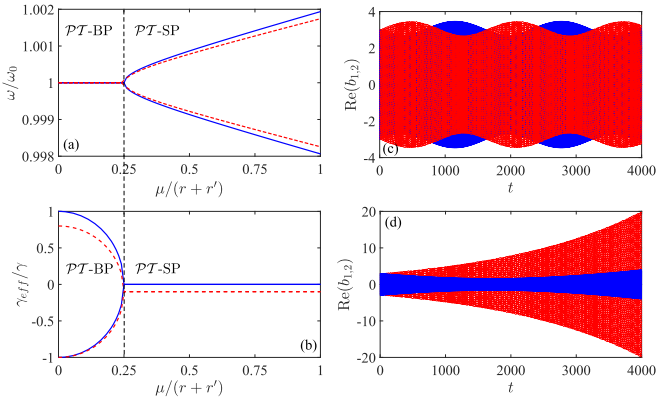

FIG. 3. (a) Real and (b) imaginary parts of the eigenfrequencies of supermodes as a function of coupling μ. Here, blue lines correspond to ideal $\mathcal{PT}$ symmetry ($\gamma = \gamma' = 0.001$). Red lines denote that the system is not strictly $\mathcal{PT}$ symmetric but has an effective dissipation rate ($\gamma' = 0.8\gamma$). (c) and (d) The dynamical behaviors of the two oscillators corresponding to $\mathcal{PT}$SP and $\mathcal{PT}$BP, respectively. Here, the unit is $\omega = 1$.

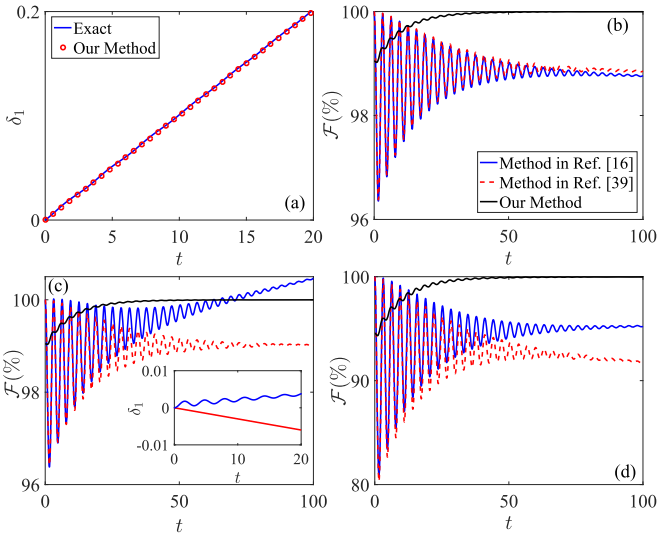

FIG. 4. (a) δ_1 given by the exact dynamic equation and our effective master equation (11). (b) and (c) Comparisons of the density matrices obtained by solving dynamic equations (11) (black solid lines), (16) (blue solid lines), and (17) (red dotted lines) under different bath phonon numbers. In (b), we set $n_{\mathrm{th}} = 0$, and in (c) $n_{\mathrm{th}} = 10$. The curves in the inset are the evolutions of δ based on exact dynamic equations (blue) and master equation (16) (red). (d) Fidelity between the system states calculated from the exact dynamic equation and effective Langevin equation (17) under $\gamma = 10^{-4}$. Here, the blue solid line and the red dotted line correspond to $n_{\mathrm{th}} = 0$ and $n_{\mathrm{th}} = 10$, respectively. In the simulations, we set $\Gamma' = \gamma - \eta\kappa$. In (b), (c), and (d), we set $\mu = 0.2\gamma$, and in (d) $G = 0.1$. The other parameters and the units are the same as those in Fig. 3.

are delivered and balanced, which is quite different from the case in $\mathcal{PT}$BP. In Fig. 3(d), we find that the gain oscillator is heated with exponentially increasing energy. However, weak coupling [$\mu = 0.1(\gamma + \gamma')$] causes the energy to be bound in one oscillator; the other oscillator cannot be heated until after a long duration of initial decrease. In $\mathcal{PT}$BP, the system can easily become unstable.

Now we compare our $\mathcal{PT}$-symmetry scheme with the others reported in previous works. According to the different gain sources, the existing implementations of $\mathcal{PT}$-symmetry schemes can be classified into the following three kinds: (i) Semiclassical gain is introduced directly into system Hamiltonian as a non-Hermitian term. The representative theoretical research of this type was reported recently in Refs. [17,20–22,36,38]. A fundamental limit in their performance is given by phenomenological gain. Quantum noise and quantum fluctuation cannot be calculated in this frame, and the second-order mechanical quantity can be estimated only by mean-field approximation after ignoring self-correlation. (ii) Quantum gain is provided by transferring a semiclassical gain to the target system via quantum coupling. A similar approach is usually adopted in the investigations of a phonon laser, and this theory can also provide a quantum dynamic equation to study system evolution. What needs to be explained is that the suitable range of the second scheme is subjected mainly to the limitation of the gain-induced dynamic modification because the origin of the gain is still semiclassical. For example, in Ref. [16], the gain system is solved by the effective master equation

$$\dot{\rho} = -i[H,\rho] + \frac{\Gamma'}{2}(n_{\mathrm{th}} + 1)\mathcal{L}[b]\rho + \frac{\Gamma'}{2}n_{\mathrm{th}}\mathcal{L}[b^\dagger]\rho. \quad (16)$$

By using an idea similar to that in Ref. [39], we can also give an effective Langevin equation for describing the gain device at the bottom of Fig. 1(b):

$$\dot{b}_1 = \left(-i\omega - \frac{\Gamma'}{2}\right)b_1 - i\mu b_2 + \sqrt{\gamma}b_{\mathrm{in}}, \quad (17)$$

where Γ' is a negative value to denote a gain rate and b_{in} is the standard Gaussian input operator. In this case, those QIP schemes that depend on the dynamic phase are still restricted. (iii) The whole system is strictly described by a complete Hamiltonian, and the gain comes up from the heating mechanism in the interior of the system. In a waveguide system, quantization amplifying medium can be approximated as a special reservoir [40]; however, it is difficult to achieve similar gain in a oscillator system.

Based on the exact dynamic equation of $\mathcal{PT}$-symmetric oscillators, we analyze the validity scope of the semiclassical approximation in the above-mentioned three types of $\mathcal{PT}$-symmetry schemes and discuss the correction of quantum dynamics caused by the quantum noise term. For a quantitative presentation, we first concentrate on $\delta_i = \langle b_i^\dagger b_i\rangle - \langle b_i^\dagger\rangle\langle b_i\rangle$, i.e., energy fluctuation of each oscillator corresponding to Hamiltonian (14). Figure 4(a) shows that the relevance of the system will continue to increase, implying that the mean-field approximation is ineffective and the non-Hermitian Hamiltonian is incapable of analyzing a pure quantum system.

Compared to the non-Hermitian Hamiltonian, the second type of $\mathcal{PT}$-symmetry schemes can also answer the evolution of quantum fluctuation, which allows us to further examine its validity by calculating corresponding fidelity. In Fig. 4(b), we present a comparison of the exact dynamic equation, effective dynamic equations (16) and (17), and our effective master equation with low bath phonon number ($n_b = 0$) and

dissipation rate ($\gamma = 10^{-5}$). We find that the results obtained from the dynamic equations (16) and (17) and our effective master equation are in good agreement ($\mathcal{F} > 98\%$) with those from the exact equation for any time scale. In Fig. 4(c), we repeat the same calculation with $n_{\rm th} = 10$, which, according to $n_{\rm th} = [\exp(\hbar\omega/k_bT) - 1]^{-1}$, corresponds to high-temperature reservoirs. We again find good agreement among the three approaches on the short-time scale, but the result based on the master equation (16) deviates from others and even exhibits nonphysical conclusion ($\mathcal{F} > 100\%$) on a long-time scale. As we mentioned above, physically, this is because Eq. (16) cannot correct the heat-flow direction, which causes the covariance matrix to have negative diagonal elements [inset of Fig. 4(c)]. Finally, in Fig. 4(d), we show the case corresponding to larger dissipation rate γ. The comparison results prove that the accuracy of dynamic equation (17) has an obvious decline trend with the increase of the dissipation rate. The reason lies in the fact that a higher dissipation rate requires a larger effective gain to balance it; correspondingly, η should also be enlarged by setting stronger coupling intensity G. The neglected shift terms will also be amplified in this case, and they will significantly affect system dynamics. Figure 4(d) illustrates that Eq. (17) will recover its accuracy when $n_{\rm th}$ is increased because the shift terms can be regarded as perturbations again when $n_{\rm th}$ is large enough. The results of Figs. 4(c) and 4(d) suggest that Eq. (17) with correct heat flow is indeed better than Eq. (16) under a wider range of parameters.

To sum up, we emphasize here again that semiclassical gain is insufficient for the study of $\mathcal{PT}$ symmetry in the quantum regime. Whether using the non-Hermitian Hamiltonian directly or transferring a semiclassical gain to the target system via quantum coupling, the obtained results are likely sometimes inaccurate, even nonphysical. In contrast, the main advantage of our scheme is to present a quantum gain that can be fully described by the effective principal equation. Therefore, the quantum fluctuation can be calculated directly and conveniently, which makes sure that our scheme has potential application for QIP.

IV. EXAMPLE OF APPLYING $\mathcal{PT}$-SYMMETRIC OSCILLATORS

We have provided a general scheme to realize $\mathcal{PT}$-symmetric oscillators in the quantum regime. This system has the interesting property of undergoing an abrupt phase transition, where the system obtains or loses its $\mathcal{PT}$ symmetry. In $\mathcal{PT}$BP, the field localization induces the dynamical accumulations in the two oscillator modes; this effect corresponds to an increasing optical-oscillator nonlinearity in an optomechanical system [41]. Previous works have used this characteristic to realize enhancements of oscillator chaos and photon blocking [17]. However, effectively using semiclassical gain in the $\mathcal{PT}$SP regime is rarely discussed in QIP. Unlike the efforts to improve coupling intensity in $\mathcal{PT}$BP, in this section, we apply our $\mathcal{PT}$-symmetric oscillators in the $\mathcal{PT}$SP regime.

Let us reexamine the master equation (11); except for reducing dissipation, the highlights of our scheme are more concentrated in its correction terms. Among them, Eq. (12) shows that the sensitivity of the system to the environment is not significantly weakened even though the effective dissipation of the oscillator is reduced. This property provides favorable support for optomechanical sensing because the decline in dissipation can also lower the sensitivity in a normal system [42]. Equation (13) describes the phonon spontaneous-generation effect, which offers the theoretic basis for the control of phonons [40].

Another perspective on our $\mathcal{PT}$ symmetry is that a negative dissipation factor and modified phonon number allow information reflux into the system. Thus, physically, the effective dissipation of undemanding $\mathcal{PT}$ symmetry is more similar to a non-Markovian system because of the elimination of the cavity field. In some special cases, a number of characteristics typical of a non-Markovian system, for example, entanglement sudden death and resurrection, may also be observed in our system [43,44], which means some QIP schemes with a non-Markovian oscillator environment may be well extended to our $\mathcal{PT}$-symmetric systems.

We also introduce an enhanced optomechanically induced transparency scheme as an example of our work. Electromagnetically induced transparency (EIT) is a remarkable interference phenomenon in quantum optics and provides a promising platform for coherent manipulation and slow-light operation. In recent years, OMIT has been widely explored both in theory and in experiment because of its better controllability [22,45–48]. However, a constraint for realizing OMIT is that OMIT windows require strong single-photon couplings that are too difficult to realize in an experiment.

Unlike the efforts to improve the single-photon coupling [41], we find that OMIT can still open in the weak-coupling regime with the help of $\mathcal{PT}$-symmetric oscillators. As shown in Fig. 5, we consider $\mathcal{PT}$-symmetric oscillators

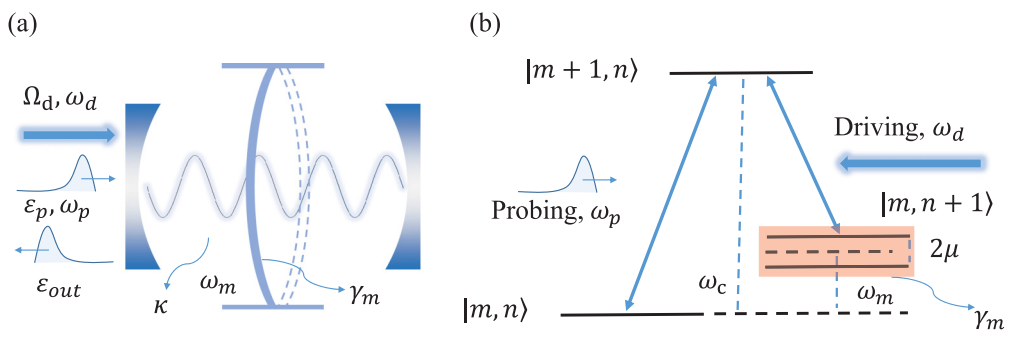

FIG. 5. (a) Optical-cavity-coupled $\mathcal{PT}$-symmetric oscillators with nonlinear radiation pressure. (b) Level diagram of the OMIT.

coupled with a cavity. The total Hamiltonian of such a system can be given by the following non-Hermitian Hamiltonian in a rotating framework:

$$H = \left(\Delta_c - i\frac{\kappa}{2}\right)a^\dagger a + \sum_{j=1,2}[\omega_m' b_j^\dagger b_j - g_0 a^\dagger a(b_j^\dagger + b_j)] + \mu(b_1^\dagger b_2 + \text{H.c.}) - i\frac{\gamma}{2}b_1^\dagger b_1 + i\frac{\gamma'}{2}b_2^\dagger b_2 + H_d + H_p, \tag{18}$$

where $H_d = i\Omega_d(a^\dagger - a)$ and $H_p = i(a^\dagger \varepsilon_p e^{-i\delta t} - a\varepsilon_p^* e^{i\delta t})$ denote, respectively, the Hamiltonians of driving and probe fields. The variables $a, b_1, b_2, \kappa, \gamma, \gamma'$, and μ are defined the same as in the previous section. γ and γ' are small compared to the coupling and the oscillator frequency. The oscillator Hamiltonian can be diagonalized in terms of the symmetric [$c = (b_1 + b_2)/\sqrt{2}$] and antisymmetric modes [$d = (b_1 - b_2)/\sqrt{2}$] as [49]

$$H = \left(\Delta_c - i\frac{\kappa}{2}\right)a^\dagger a + \left(\omega_m - i\frac{\gamma_m}{2}\right)c^\dagger c - ga^\dagger a(c^\dagger + c) + H_d + H_p. \tag{19}$$

Here, we have already set $g = \sqrt{2}g_0$, $\omega_m = \omega_m' + \mu$ and $\gamma_m = (\gamma - \gamma')/2$ for convenience. Note that the antisymmetric mode has also been neglected because it has no direct interaction with the optical mode. The steady-state solution of such a system can be expanded to contain many Fourier components. Under the limitation of weak strength of the probe field, each operator in Eq. (19) will have the following form: $o = o_0 + o_+\varepsilon_p e^{-i\delta t} + o_-\varepsilon_p^* e^{i\delta t}$ by neglecting the high-order terms of ε_p [48,50,51]. Substituting this relation into the semiclassical Langevin equations [52,53] and using the steady-state condition, the optical field can be solved as

$$a_+ = \frac{\left\{(\omega_m^2 - \delta^2 - i\delta\gamma_m/2)\left[-i(\Delta + \delta) + \frac{\kappa}{2}\right] + \beta\right\}}{(\omega_m^2 - \delta^2 - i\delta\gamma_m/2)\left[i(\Delta - \delta) + \frac{\kappa}{2}\right]\left[-i(\Delta + \delta) + \frac{\kappa}{2}\right] + i2\beta\Delta} \tag{20}$$

by using the input-output relation $\varepsilon_{\text{out}}(t) + \varepsilon_p e^{-i\delta t} + \Omega_d = \kappa a$. In the above expression, $\beta = i2g_0\omega_m x_0$ is a characteristic parameter proportional to the photon number. Like in previous works, we concentrate on the behaviors of a_+ and define $\chi = \kappa a_+$ to describe the response of the cavity optomechanical system to the probe field. According to the absorption and dispersion theory, one can determine that the real and imagery parts of χ represent, respectively, the behaviors of absorption and dispersion [46], and an OMIT window should satisfy $\text{Re}(\chi) \to 0$ and $\text{Im}(\chi) \to 0$ simultaneously.

In Figs. 6(a) and 6(b), we plot the behaviors of $\text{Re}(\chi) \to 0$ and $\text{Im}(\chi) \to 0$, respectively, for both $\mathcal{PT}$-symmetric oscillators and ordinary oscillators. It can be known that the $\mathcal{PT}$-symmetric case offers an obvious transparent window at the modified sideband $\delta = \omega_p - \omega_d = \omega_m' + \mu$. This OMIT phenomenon emerges in the weak-coupling regime but will not exist if the oscillator dissipation is not balanced by gain. In Figs. 6(c) and 6(d), one can find that for a similar transparent window, the single-photon coupling intensity in the dissipation system must be amplified approximately 40 times, which is a harsh condition for an experiment. From this point of view, we conclude that the $\mathcal{PT}$-symmetric oscillators can indeed enhance the OMIT phenomenon in the weak-coupling regime.

Now we discuss the physical mechanism corresponding to $\mathcal{PT}$-symmetric oscillator-enhanced OMIT. The underlying physics of OMIT are formally similar to those of ordinary EIT in an atomic system. Huang and Agarwal [45] discussed this relation and sketched three conditions for OMIT to occur: (i) The driving frequency must be set in the red sideband, (ii) the optical-field loss needs to be much greater than that of oscillator dissipation, and (iii) the steady-state of oscillator displacement cannot be zero. The first and third conditions are combined to ensure a similar energy-level structure with a Λ-type atom [see Fig. 5(b)], and the first and second conditions protect the interference between driving and probe fields.

For a normal optomechanical system, oscillator displacement is proportional to the cavity photon number, which causes there to be a conflict between the last two conditions in this case. A larger cavity dissipation satisfying condition (ii) will reduce the photon number significantly, indicating that condition (iii) is violated. With the same intercavity photon number, the only way to push the oscillator farther from its equilibrium position is to try to further enhance

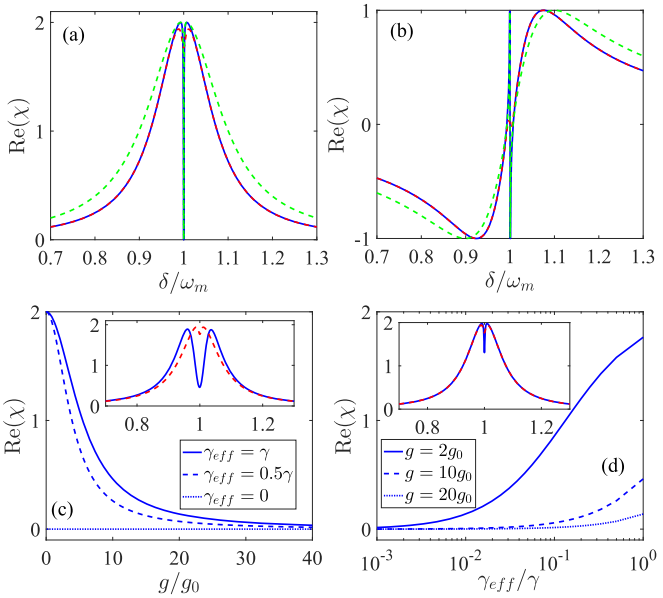

FIG. 6. (a) Real and (b) imaginary parts of χ corresponding to $\mathcal{PT}$-symmetric oscillators (blue and green lines) and dissipative oscillators (red lines). (c) and (d) Depths of transparent windows with varied single-photon coupling intensity g and oscillator dissipation rate γ_m. The insets illustrate the changes of absorption spectra under different γ_{eff} [in (c)] and g [in (d)]. In this simulation, the parameter unit is set as $\Delta = \omega_m = 1$, and other parameters are $g_0 = 2.5\times10^{-4}$, $E = 10$, $\kappa = 0.15$, and $\gamma = 0.02$. In (a) and (b), the corresponding single-photon coupling is $2g_0$, and green lines are under $\kappa = 0.2$.

optical-oscillator coupling. This is the reason why previous works have required strong single-photon coupling intensity to satisfy the two contradictory OMIT conditions.

However, if we use $\mathcal{PT}$-symmetric oscillators instead of dissipative oscillators in the OMIT system, oscillator dissipation is reduced effectively in the $\mathcal{PT}$SP regime. Thus, the requested cavity dissipation can also be reduced, which leads to there being enough intercavity photons to ensure nonzero steady-state oscillator displacement with weak coupling. In other words, the contradictory OMIT conditions can be well met simultaneously, which is why the $\mathcal{PT}$-symmetric oscillators can enhance OMIT.

V. DISCUSSION

Now we give the feasibility analyses regarding our parameters used in the above discussions. First, for the linearization, good correspondence between the nonlinear Hamiltonian (1) and linear Hamiltonian (3) has been introduced in recent experimental studies. Recent experiments have successfully realized optomechanical cooling based on the linear Hamiltonian (3) [54,55], and the latest theoretical work also noted that the linearized coupling coefficient G can even be controlled as a control field [31]. In addition to the oscillator gain, the BS coupling between the oscillators has also been widely discussed [24,56,57]. Therefore, the heating effect and the $\mathcal{PT}$-symmetric scheme in our work can be easily realized via experiments.

In the OMIT part, the dimensionless parameters are adopted according to the existing experimental parameters of OMIT and chaos in an optomechanical system, i.e., $\omega_d + \Delta_c = 195$ THz (1573 nm), $\omega_m/2\pi = 3.68$ GHz, $\kappa/2\pi = 500$ MHz, and $g_0/2\pi = 910$ kHz, which correspond to $\kappa/\omega_m = 0.1359 \simeq 0.15$ and $g_0/\omega_m = 2.473\times10^{-4} \simeq 2.5\times10^{-4}$, respectively [54,58]. As discussed above, our OMIT scheme does not require an oscillator with a high Q factor. Therefore, some low-Q-factor oscillators (for example, the oscillator reported in Ref. [59]) can also be utilized to realize OMIT. Although realizing strong optomechanical interaction requires sacrificing the Q factor of the oscillator in some experiments, our scheme can alleviate this contradiction to a certain extent, which is equivalent to indirectly improving the system coupling. In the comparison part, the relation $\gamma/\omega_m \sim 10^{-3}, 10^{-4}$ has also been established in many recent experiments [23,60]. In summary, we think that the parameters in our scheme are feasible.

In summary, we have proposed a theoretical scheme to realize the $\mathcal{PT}$-symmetric oscillators in the quantum regime. The oscillator gain originates from an optomechanical system corresponding to a heating effect, and we can provide a quantum description for such a gain by eliminating the cavity modes, which is quite different from those in previous works, in which the gain was considered only as a semiclassical amplification. We also prove this advantage by comparing our method with the previous schemes. Subsequently, we present an effective master equation for such a gain system containing effective dissipation, the bath phonon number, and the initial state. This master equation allows us to obtain a complete quantum description of the $\mathcal{PT}$-symmetric oscillators, indicating that some QIP schemes can be well optimized by using our $\mathcal{PT}$-symmetric oscillator even if the semiclassical gain is powerless. As an example, we have shown how to enhance optomechanically induced transparency based on the $\mathcal{PT}$-symmetric oscillators. The results illustrate that $\mathrm{Re}(\chi) \sim 0$ and $\mathrm{Im}(\chi) \sim 0$ are easily satisfied even if both driving and nonlinear coupling are extremely weak. We thus believe the scheme proposed here may provide a promising choice for the unachievable strong nonlinear coupling in quantum optical devices and is of potential application for coherent manipulation, slow-light operation, and other utilizations in QIP.

We also note that the gain oscillator and the dissipative oscillator coconstruct a closed-like system, implying that an additional oscillator may be regarded as a special non-Markovian environment of the dissipative oscillator. In a recent experiment [61], a narrowband spectral density was observed, and the corresponding dynamic property was very similar to a single-mode environment [30]. Therefore, we can predict that most QIP schemes with a non-Markovian oscillator environment (e.g., Refs. [30,43]) can be well extended to our $\mathcal{PT}$-symmetric systems. The possibility of the idea will be further verified in subsequent studies.

ACKNOWLEDGMENTS

The authors thank Dr. J. Cheng, W.-z. Zhang, and Y. Zhang for the useful discussions. This research was supported by the National Natural Science Foundation of China (Grants No. 11574041 and No. 11175033).

APPENDIX A: LINEARIZED OPTOMECHANICAL HAMILTONIAN

The splittings of operators $\hat{a}(t) = \alpha(t) + a(t)$ and $\hat{b}(t) = \beta(t) + b(t)$ can be regarded as a displacement transformation on the system dynamic operators, where α and β are c numbers denoting the displacements of the optical and mechanical modes; a and b are the displaced operators representing the quantum fluctuations of the optical and mechanical modes around their classical values. By separating the classical and quantum components, the classical Langevin equations are written as

$$\dot{\alpha} = \left(i\Delta' - \frac{\kappa}{2}\right)\alpha - i\Omega, \quad \dot{\beta} = \left(-i\omega_m - \frac{\gamma}{2}\right)\beta - ig|\alpha|^2. \tag{A1}$$

If the optomechanical coupling is quite weak in the quantum regime, the motion of the oscillator and optical field can be regarded as perturbations on their respective steady states. Under this conditions, we obtain

$$\alpha_{t\to\infty} = \frac{i\Omega}{\left(i\Delta' - \frac{\kappa}{2}\right)}, \quad \beta_{t\to\infty} = \frac{ig|\alpha|^2}{\left(-i\omega_m - \frac{\gamma}{2}\right)}, \tag{A2}$$

and the dynamics of a and b satisfy

$$\dot{a} = \left(i\Delta' - \frac{\kappa}{2}\right)a - ig\alpha(b + b^\dagger) - iga(b + b^\dagger) - \hat{\xi},$$
$$\dot{b} = \left(-i\omega_m - \frac{\gamma}{2}\right)b - ig(\alpha^* a + \alpha a^\dagger) - iga^\dagger a - \sqrt{\gamma}b_{\mathrm{in}}. \tag{A3}$$

Under a strong driving condition, the nonlinear terms $iga(b+b^\dagger)$ and $iga^\dagger a$ can be neglected and the linearized Hamiltonian $H=-\Delta' a^\dagger a+\omega b^\dagger b+(Ga^\dagger+G^* a)(b^\dagger+b)$ can be obtained, where $G=\alpha g$ is the linearized optomechanical coupling strength. After a rotating-wave approximation, we finally get

$$H=-\Delta' a^\dagger a+\omega b^\dagger b+Ga^\dagger b^\dagger+G^* ab \tag{A4}$$

under the blue-sideband condition $\Delta'>0$. Equation (A4) is exactly Eq. (3) in the main text.

APPENDIX B: DERIVATION OF THE OSCILLATOR EFFECTIVE GAIN

With the master equation (4) in the main text, we first consider the first-order parts in Eq. (5), and these equations can be formally integrated as

$$\begin{aligned}\langle a\rangle(t)&=\langle a\rangle_{t_0}\exp\left(i\Delta-\frac{\kappa}{2}\right)t+\exp\left(i\Delta t-\frac{\kappa}{2}t\right)\int_0^t -iG\langle b\rangle^*(\tau)\exp\left(-i\Delta\tau+\frac{\kappa}{2}\tau\right)d\tau,\\ \langle b\rangle^*(t)&=\langle b\rangle^*_{t_0}\exp\left(i\omega_m-\frac{\gamma}{2}\right)t+\exp\left(i\omega_m t-\frac{\gamma}{2}t\right)\int_0^t iG\langle a\rangle(\tau)\exp\left(-i\omega_m\tau+\frac{\gamma}{2}\tau\right)d\tau.\end{aligned} \tag{B1}$$

In the case of $\Delta-\omega_m\gg G$ or $\kappa\gg\gamma$, the optical field is a high-frequency oscillation term or a highly dissipative term. Then the mode a can be regarded as a perturbation of the mechanical mode. The slight influence by a can be neglected, and the following approximated expression can be further obtained: $\langle b\rangle^*(t)=\langle b\rangle^*_{t_0}\exp(i\omega_m-\gamma/2)t$. Substituting it into $\langle a\rangle(t)$ in Eq. (B1) and finishing the integral inside it, an approximate solution of the optical mode can be expressed as

$$\langle a\rangle(t)\simeq\frac{-2iG}{2i(\omega_m-\Delta)+\kappa-\gamma}\langle b\rangle^*_{t_0}\exp\left(i\omega_m-\frac{\gamma}{2}\right)t\simeq\frac{-2iG}{2i(\omega_m-\Delta)+\kappa}\langle b\rangle^*(t) \tag{B2}$$

under the condition $\Delta-\omega_m\gg G$ or $\kappa\gg\gamma$. Substituting this approximate solution into Eq. (5), we can get the following effective first-order expectation value equation:

$$\frac{d}{dt}\langle b\rangle=\left[-i\left(\omega_m+\frac{4|G|^2(\Delta-\omega_m)}{4(\Delta-\omega_m)^2+\kappa^2}\right)-\frac{1}{2}\left(\gamma-\frac{4|G|^2\kappa}{4(\Delta-\omega_m)^2+\kappa^2}\right)\right]\langle b\rangle. \tag{B3}$$

Equation (B3) is exactly the same as Eq. (8) in the main text. Now we consider the second-order mechanical quantities. Like for the case of the first order and after substituting the approximate solutions of $\langle a^\dagger a\rangle(t)$ and $\langle b^\dagger b\rangle(t)$ into $\langle ab\rangle(t)$, we obtain

$$\langle ab\rangle(t)\simeq -iG\left\{\frac{\langle b^\dagger b\rangle(t)}{-i(\Delta-\omega_m)+\kappa/2}+\frac{1}{-i(\Delta-\omega_m)+\kappa/2}\right\}+\mathcal{O}(t), \tag{B4}$$

where

$$\begin{aligned}\mathcal{O}(t)=&\langle ab\rangle_{t_0}\exp\left[i(\Delta-\omega_m)-\frac{\kappa}{2}\right]t+\frac{-iG}{-i(\Delta-\omega_m)+\kappa/2}\left\{-\langle b^\dagger b\rangle_{t_0}\exp\left[i(\Delta-\omega_m)-\frac{\kappa}{2}\right]t\right\}\\&+\frac{-iG}{-i(\Delta-\omega_m)-\kappa/2}\left\{\langle a^\dagger a\rangle_{t_0}\exp(-\kappa t)-\langle a^\dagger a\rangle_{t_0}\exp\left[i(\Delta-\omega_m)-\frac{\kappa}{2}\right]t\right\}.\end{aligned} \tag{B5}$$

We first neglect the $\mathcal{O}(t)$ term in Eq. (B4) because it is a time-oscillation term with dissipation; then the modified second-order equation is exactly the same as Eq. (9) in the main text, and we find that the effective dissipation in this case is self-consistent with the first-order effective dissipation. By using it, we have

$$\langle b^\dagger b\rangle(t)=\langle b^\dagger b\rangle_{t_0}\exp(-\Gamma_{\rm eff})t+\exp(-\Gamma_{\rm eff}t)\int_0^t\{-i[G\mathcal{O}^*(\tau)-G^*\mathcal{O}]+\Gamma_{\rm eff}n'_{\rm th}\}\exp(\Gamma_{\rm eff}\tau)d\tau. \tag{B6}$$

After completing integration in the above expression, we achieve the following relationship:

$$\int_0^t\{-i[G\mathcal{O}^*(\tau)-G^*\mathcal{O}]\}\exp(\Gamma_{\rm eff}\tau)d\tau\simeq\frac{4|G|^2\langle a^\dagger a\rangle_{t_0}}{4(\Delta-\omega_m)^2+\kappa^2}-\frac{8G(\Delta-\omega_m)\langle ab\rangle_{t_0}}{4(\Delta-\omega_m)^2+\kappa^2}+\frac{8|G|^2\langle b^\dagger b\rangle_{t_0}}{4(\Delta-\omega_m)^2+\kappa^2}. \tag{B7}$$

Here, the final equal relationship in Eq. (B7) requires that G and $\langle ab\rangle(0)$ are both real and $\kappa^2/4\ll(\Delta-\omega_m)^2$. Then substituting Eq. (B7) into Eq. (B6), we obtain

$$\langle b^\dagger b\rangle(t)=\langle b^\dagger b\rangle'_{t_0}\exp(-\Gamma_{\rm eff})t+\exp(-\Gamma_{\rm eff}t)\int_0^t\{\Gamma_{\rm eff}n'_{\rm th}\}\exp(\Gamma_{\rm eff}\tau)d\tau, \tag{B8}$$

and

$$\langle b^\dagger b\rangle'_{t_0}=\left(1+\frac{8|G|^2}{4(\Delta-\omega_m)^2+\kappa^2}\right)\langle b^\dagger b\rangle(0)+\frac{4|G|^2\langle a^\dagger a\rangle(0)}{4(\Delta-\omega_m)^2+\kappa^2}-\frac{8G(\Delta-\omega_m)\langle ab\rangle(0)}{4(\Delta-\omega_m)^2+\kappa^2} \tag{B9}$$

can be considered a modified initial condition of the oscillator phonon number. Correspondingly, we assume $\langle b\rangle'_{t_0} = \sqrt{\langle b^\dagger b\rangle'_{t_0}}$ for convenience. Equation (B9) is exactly the same as the modified initial condition in Eq. (13) in the main text.

[1] C. E. Rüter, K. G. Makris, R. El-Ganainy, D. N. Christodoulides, M. Segev, and D. Kip, Nat. Phys. **6**, 192 (2010).
[2] L. Chang, X. Jiang, S. Hua, C. Yang, J. Wen, L. Jiang, G. Li, G. Wang, and M. Xiao, Nat. Photon. **8**, 524 (2014).
[3] L. Feng, Z. J. Wong, R. M. Ma, Y. Wang, and X. Zhang, Science **346**, 972 (2014).
[4] X. Luo, J. Huang, H. Zhong, X. Qin, Q. Xie, Y. S. Kivshar, and C. Lee, Phys. Rev. Lett. **110**, 243902 (2013).
[5] C. M. Bender and S. Boettcher, Phys. Rev. Lett. **80**, 5243 (1998).
[6] C. M. Bender, D. C. Brody, and H. F. Jones, Phys. Rev. Lett. **89**, 270401 (2002).
[7] S. Malzard, C. Poli, and H. Schomerus, Phys. Rev. Lett. **115**, 200402 (2015).
[8] A. Demirkaya, D. J. Frantzeskakis, P. G. Kevrekidis, A. Saxena, and A. Stefanov, Phys. Rev. E **88**, 023203 (2013).
[9] P. G. Kevrekidis, J. Cuevas–Maraver, A. Saxena, F. Cooper, and A. Khare, Phys. Rev. E **92**, 042901 (2015).
[10] B. Peng, Ş. K. Özdemir, F. Lei, F. Monifi, M. Gianfreda, G. L. Long, S. Fan, F. Nori, C. M. Bender, and L. Yang, Nat. Phys. **10**, 394 (2014).
[11] A. Regensburger, C. Bersch, M. Miri, G. Onishchukov, D. N. Christodoulides, and U. Peschel, Nature (London) **488**, 167 (2012).
[12] L. Feng, M. Ayache, J. Huang, Y. Xu, M. H. Lu, Y. F. Chen, Y. Fainman, and A. Scherer, Science **333**, 729 (2011).
[13] B. Peng, Ş. K. Özdemir, S. Rotter, H. Yilmaz, M. Liertzer, F. Monifi, C. M. Benderm, F. Nori, and L. Yang, Science **346**, 328 (2014).
[14] C. M. Bender, Rep. Prog. Phys. **70**, 947 (2007).
[15] S. K. Gupta and A. K. Sarma, Commun. Nonlinear Sci. Numer. Simul. **36**, 141 (2016).
[16] J. Li, R. Yu, and Y. Wu, Phys. Rev. A **92**, 053837 (2015).
[17] X. Y. Lü, H. Jing, J. Y. Ma, and Y. Wu, Phys. Rev. Lett. **114**, 253601 (2015).
[18] S. Savoia, G. Castaldi, V. Galdi, A. Alù, and N. Engheta, Phys. Rev. B **91**, 115114 (2015).
[19] A. Galda and V. M. Vinokur, Phys. Rev. B **94**, 020408(R) (2016).
[20] S. Phang, A. Vukovic, S. C. Creagh, T. M. Benson, P. D. Sewell, and G. Gradoni, Opt. Express **23**, 11493 (2015).
[21] J. Li, X. Zhan, C. Ding, D. Zhang, and Y. Wu, Phys. Rev. A **92**, 043830 (2015).
[22] H. Jing, Ş. K. Özdemir, Z. Geng, J. Zhang, X. Y. Lü, B. Peng, L. Yang, and F. Nori, Sci. Rep. **5**, 9663 (2015).
[23] A. Mari and J. Eisert, Phys. Rev. Lett. **103**, 213603 (2009).
[24] A. Mari, A. Farace, N. Didier, V. Giovannetti, and R. Fazio, Phys. Rev. Lett. **111**, 103605 (2013).
[25] D. Vitali, S. Gigan, A. Ferreira, H. R. Böhm, P. Tombesi, A. Guerreiro, V. Vedral, A. Zeilinger, and M. Aspelmeyer, Phys. Rev. Lett. **98**, 030405 (2007).
[26] U. R. Fischer and M. K. Kang, Phys. Rev. Lett. **115**, 260404 (2015).
[27] M. A. Hall, J. B. Altepeter, and P. Kumar, Phys. Rev. Lett. **106**, 053901 (2011).
[28] M. Aspelmeyer, T. J. Kippenberg, and F. Marquardt, Rev. Mod. Phys. **86**, 1391 (2014).
[29] Y. C. Liu, Y. F. Xiao, X. Luan, and C. W. Wong, Phys. Rev. Lett. **110**, 153606 (2013).
[30] W. Z. Zhang, J. Cheng, W. D. Li, and L. Zhou, Phys. Rev. A **93**, 063853 (2016).
[31] J. F. Triana, A. F. Estrada, and L. A. Pachón, Phys. Rev. Lett. **116**, 183602 (2016).
[32] X. W. Xu, Y. X. Liu, C. P. Sun, and Y. Li, Phys. Rev. A **92**, 013852 (2015).
[33] Z. P. Liu, J. Zhang, Ş. K. Özdemir, B. Peng, H. Jing, X. Y. Lü, C. W. Li, L. Yang, F. Nori, and Y. X. Liu, Phys. Rev. Lett. **117**, 110802 (2016).
[34] H. Scutaru, J. Phys. A **31**, 3659 (1998).
[35] A. Isar, Phys. Part. Nucl. Lett. **6**, 567 (2009).
[36] C. M. Bender, M. Gianfreda, Ş. K. Özdemir, B. Peng, and L. Yang, Phys. Rev. A **88**, 062111 (2013).
[37] S. Karthiga, V. K. Chandrasekar, M. Senthilvelan, and M. Lakshmanan, Phys. Rev. A **93**, 012102 (2016).
[38] B. He, L. Yang, Z. Zhang, and M. Xiao, Phys. Rev. A **91**, 033830 (2015).
[39] H. Jing, Ş. K. Özdemir, X. Y. Lü, J. Zhang, L. Yang, and F. Nori, Phys. Rev. Lett. **113**, 053604 (2014).
[40] G. S. Agarwal and K. Qu, Phys. Rev. A **85**, 031802(R) (2012).
[41] Y. C. Liu, Y. F. Xiao, Y. L. Chen, X. C. Yu, and Q. Gong, Phys. Rev. Lett. **111**, 083601 (2013).
[42] W. Z. Zhang, Y. Han, B. Xiong, and L. Zhou, arXiv:1609.05491.
[43] J. Cheng, W. Z. Zhang, L. Zhou, and W. Zhang, Sci. Rep. **6**, 23678 (2016).
[44] H. Krauter, C. A. Muschik, K. Jensen, W. Wasilewski, J. M. Petersen, J. I. Cirac, and E. S. Polzik, Phys. Rev. Lett. **107**, 080503 (2011).
[45] S. Huang and G. S. Agarwal, Phys. Rev. A **83**, 023823 (2011).
[46] G. S. Agarwal and S. Huang, Phys. Rev. A **81**, 041803(R) (2010).
[47] Y. Guo, K. Li, W. Nie, and Y. Li, Phys. Rev. A **90**, 053841 (2014).
[48] W. Li, Y. Jiang, C. Li, and H. Song, Sci. Rep. **6**, 31095 (2016).
[49] Y. L. Liu and Y. X. Liu, arXiv:1609.02722. The accurate eigenvectors should correspond to $\lambda_\pm$ in Eq. (15). Because $\gamma \ll \mu, \omega_m$, we approximately consider that $\lambda_\pm = \omega_m \pm \mu$ and neglect the term $c^\dagger d$ + H.c. here.
[50] H. Wang, H. C. Sun, J. Zhang, and Y. X. Liu, Sci. China Phys. Mech. Astron. **55**, 2264 (2012).
[51] A. Sohail, Y. Zhang, J. Zhang, and C. S. Yu, Sci. Rep. **6**, 28830 (2016).
[52] G. Wang, L. Huang, Y. C. Lai, and C. Grebogi, Phys. Rev. Lett. **112**, 110406 (2014).
[53] W. Li, C. Li, and H. Song, Phys. Rev. E **93**, 062221 (2016).
[54] J. Chan, T. P. Mayer-Alegre, A. H. Safavi-Naeini, J. T. Hill, A. Krause, S. Gröblacher, M. Aspelmeyer, and O. Painter, Nature (London) **478**, 89 (2011).
[55] M. Eichenfield, J. Chan, R. M. Camacho, K. J. Vahala, and O. Painter, Nature (London) **462**, 78 (2009).
[56] M. Ludwig and F. Marquardt, Phys. Rev. Lett. **111**, 073603 (2013).

[57] V. Ameri, M. Eghbali-Arani, A. Mari, A. Farace, F. Kheirandish, V. Giovannetti, and R. Fazio, Phys. Rev. A **91**, 012301 (2015).

[58] F. Massel, T. T. Heikkilä, J. M. Pirkkalainen, S. U. Cho, H. Saloniemi, P. J. Hakonen, and M. A. Sillanpää, Nature (London) **480**, 351 (2011).

[59] K. W. Murch, K. L. Moore, S. Gupta, and D. M. Stamper-Kurn, Nat. Phys. **4**, 561 (2008).

[60] F. Marquardt and S. M. Girvin, Physics **2**, 40 (2009).

[61] S. Gröblacher, A. Trubarov, N. Prigge, G. D. Cole, M. Aspelmeyer, and J. Eisert, Nat. Commun. **6**, 7606 (2015).